View metadata, citation and similar papers at core.ac.uk brought to you by CORE

**FACTA UNIVERSITATIS**
Series:**Electronics and Energetics** Vol. 31, N° 1, March 2018, pp. 89 - 100
https://doi.org/10.2298/FUEE1801089A

# INTRODUCING A NOVEL HIGH-EFFICIENCY ARC LESS HETEROUNCTION DJ SOLAR CELL

**Sobhan Abasian[1,2], Reza Sabbaghi-Nadooshan[1]**

[1]Electrical Engineering Department, Islamic Azad University, Central Tehran Branch, Tehran, Iran
[2]Ahvaz Electricity Distribution Company, Ahvaz, Iran

**Abstract**. *The present study was undertaken to examine the structure and performance of hetero junctions on the fill factor, short circuit current and open circuit voltage of aInGaP/GaAsdual-junction solar cell. This goal of this work was to reduce recombination in the bottom cell so that the electrons and holes produced in the top cell with the lowest recombination participate in the output current. Semiconductors with a high bandwidth from the ɪɪɪv group were studied in order to obtain a high open circuit voltage. By observing mobility and lattice constant semiconductors ($Al_{0.52}In_{0.48}P$, GaAs and $In_{0.49}Ga_{0.51}P$), it was concluded that the semiconductor $Al_{0.52}In_{0.48}P$ has high electron mobility and hole mobility and that the lattice constant matched to the GaAs semiconductor can be effective in reducing recombination. The cathode current and absorbed photons show that the composition InGaP/AlInP increased the number of charge carriers in the top cell. The structure of InGaP-AlInP/GaAs-AlInP was obtained by inserting an InGaP-AlInP heterojunction at the top and GaAs-AlInP heterojunction at the bottom of aInGaP/GaAs dual-junction cell. For this structure, short circuit current ($J_{SC}$) = 22.96 mA/cm$^2$, open circuit voltage (Voc) = 2.72 V, fill factor (FF) = 93.26% and efficiency($\eta$)= 58.28% were obtained under AM1.5 (1 sun) of radiation.*

**Key words**: *Solar cell, Dual-junction, heterojunction, ARC less*

## 1. INTRODUCTION

The growing demand for energy and increasing environmental pollution have attracted attention of researchers and investors to the renewable energy sector. Solar energy is a renewable resource that produces electricity through photovoltaic solar cells. Much research has been conducted to increase the efficiency of solar cells by using III-V compound semiconductors by increasing the number of p-n junctions for greater absorption of sunlight.

Hutchby et al. presented the first AlGaAs/GaAs dual-junction cell [1]. Lueck et al. obtained an efficiency of 23.6% by placing the InGaP/GaAs dual-junction cell on GaAs

Received March 30, 2017; received in revised form July 14, 2017
**Corresponding author:** Reza Sabbaghi-Nadooshan
Electrical Engineering Department, Islamic Azad University, Central Tehran Branch, Tehran, Iran
(E-mail: sobhan_aba@yahoo.com)

under radiation at AM1.5 (1 sun) [2]. Leem et al. designed aInGaP/GaAs dual-junction cell with a InGaP/InGaP tunnel diode. The efficiency of this cell was 25.14% under radiation of AM1.5 (1 sun) [3]. Singh et al. obtained efficiency of 32.196% under radiation of AM1.5 (1 sun) by inserting $In_{0.5}(Al_{0.7}Ga_{0.3})_{0.5}P$ into the back surface field (BSF) layer at the bottom of a InGaP/GaAs dual-junction cell [4]. Nayak et al. reported a efficiency of 39.15% under radiation of AM1.5 (1000 sun) by creating an extra electric field using two back surface field (BSF) layers [5]. Abbasian et al. used semiconductors in $_{0.5}(Al_{0.7}Ga_{0.3})_{0.5}P$ at low irradiation and arrived at 53.51% efficiency under radiation of AM1.5G (1 sun) [6].

The current study obtained a favorable structure for InGaP-AlInP/GaAs-AlInP dual-junction cells using heterojunctions. The performance of the proposed cell was simulated using the Silvaco Atlas under the standard AM1.5 spectrum and the values obtained for efficiency(η), fill factor (FF), open circuit voltage (Voc) and short circuit current ($J_{SC}$) were compared with those from previous works.

In the rest of the paper, section 2 describes the solar cell model. Section 3 shows and discusses the results, and section 4 compares the results with other works. Finally, section 5 concludes the paper.

## 2. Modeling Solar Cells

### 2.1. Structure of multi-junction cells

In multi-junction cells, each cell consists of a window layer and p-n junction layer and back surface field (BSF) layer. Cells that absorb wave length proportional to a semiconductor are used in the p-n junction and are connected by a tunnel junction. The window layer has a high band gap that allows photons to pass like a transparent substance and causes maximum absorption of sunlight.

Charge carriers produced by irradiation of photons are separated at the p-n junction and back surface field (BSF) layer, which reduces surface recombination of charge carriers by producing an electric field. The tunnel junction provides conditions for passage of the charge carriers from a route having low resistance by creating a low-width discharge area [4-8]. Figure 1 shows a dual-junction solar cell.

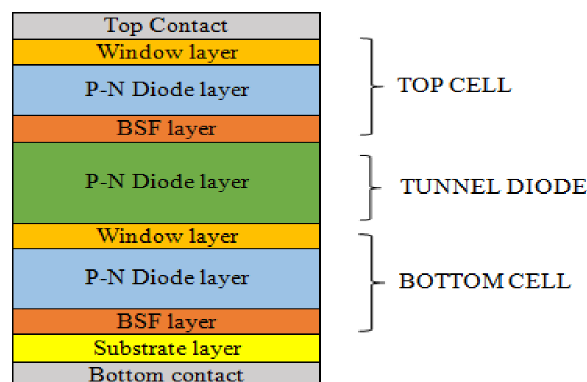


**Fig. 1** Layers of dual-junction solar cell

### 2.2. Selection of materials for heterojunction

Heterojunctions are used to apply the properties of different materials at a p-n junction. Materials with a high bandwidth such as $Al_{0.52}In_{0.48}P$ and GaAs were used to reduce the effect of recombination in the GaAs emitter layer and to increase the open circuit voltage [9]. M.R. Islam et al [10] showed that the combination of InGaP/AlInP increased the life time of the carriers, reduced recombination and increased the short circuit current. Table 1 shows that the electron and hole mobility of $Al_{0.52}In_{0.48}P$ is suitable for combination with GaAs and $In_{0.49}Ga_{0.51}P$ semiconductor.

The lattice constant is an important parameter in combination with different semiconductors. Table 1 shows that $In_{0.5}(Al_{0.7}Ga_{0.3})_{0.5}P$, $In_{0.49}Ga_{0.51}P$ and $Al_{0.52}In_{0.48}P$ prevent trap levels in the structure with similar lattice constant. To increase the efficiency in the InGaP/GaAs dual-junction base cell [5], InGaP/AlInP and GaAs/AlInP heterojunctions were placed at the top and bottom of the cells, respectively. Figure 2 shows the proposed structure to increase the efficiency of the InGaP/GaAs dual junction cell. As can be seen, the cell high-band gap the semiconductor selected the window layer to allow the light to pass through and prevent surface recombination. The p-n junction in the top cell absorbed the shorter wavelengths of the light spectrum and the BSF layers blocked the recombination of electrons and holes generated in the top cell. The top and bottom cells were connected by a GaAs tunnel junction with a band gap of 1.4ev. The bottom cell absorbed long wavelengths of sunlight and cross charge carriers generated in the top cell increased efficiency in the dual-junction cell.

**Table 1** Major parameters for the ternary ($Al_{0.52}In_{0.48}P$ , $In_{0.49}Ga_{0.51}P$) and quaternary $In_{0.5}(Al_{0.7}Ga_{0.3})_{0.5}P$ lattice matched to GaAs materials used in this design [11-14].

| Material | GaAs | InGaP | InAlGaP | AlInP |
|---|---|---|---|---|
| Band gap Eg (eV) @300 K | 1.42 | 1.9 | 2.3 | 2.4 |
| Lattice constant α (Å) | 5.65 | 5.65 | 5.65 | 5.65 |
| Permittivity (es/eo) | 13.1 | 11.6 | 11.7 | 11.7 |
| Affinity (eV) | 4.07 | 4.16 | 4.2 | 4.2 |
| Heavy e- effective mass ($m_e^*/m_0$) | 0.063 | 3 | 2.85 | 2.65 |
| Heavy h + effective mass ($m_h^*/m_0$) | 0.5 | 0. 64 | 0. 64 | 0.64 |
| e- mobility MUN ($cm^2/V\times s$) | 8800 | 1945 | 2150 | 2291 |
| h + mobility MUP ($cm^2/V\times s$) | 400 | 141 | 141 | 142 |
| e- density of states $N_C$ ($cm^{-3}$) | 4.7e+17 | 1.30e+20 | 1.20e+20 | 1.08e+20 |
| h + density of states $N_V$ ($cm^{-3}$) | 7.0e+18 | 1.28e+19 | 1.28e+19 | 1.28e+19 |

Anode Contact

| Thickness | Layer | Material | Doping | |
|---|---|---|---|---|
| 0.030μm | Window | $In_{0.5}(Al_{0.7}Ga_{0.5})_{0.5}P$ | $P=2e18\ cm^{-3}$ | Top InGaP-AlInP Cell |
| 0.050μm | Emitter | $In_{0.49}Ga_{0.51}P$ | $P=2e19\ cm^{-3}$ | |
| 0.550μm | Base | $Al_{0.5}In_{0.5}P$ | $n=7e16\ cm^{-3}$ | |
| 0.030μm | BSF | $In_{0.5}(Al_{0.7}Ga_{0.3})_{0.5}P$ | $n=2e17\ cm^{-3}$ | |
| 0.030μm | BSF | $In_{0.5}(Al_{0.7}Ga_{0.3})_{0.5}P$ | $n=2e18\ cm^{-3}$ | |
| 0.025μm | Tunnel Diode | GaAs | $n=5e19\ cm^{-3}$ | GaAs Tunnel Diode |
| 0.025μm | Tunnel Diode | GaAs | $P=3e19\ cm^{-3}$ | |
| 0.040μm | Window | $In_{0.49}Ga_{0.51}P$ | $P=3e18\ cm^{-3}$ | Bottom GaAs-AlInP Cell |
| 0.300μm | Emitter | GaAs | $p=2e18\ cm^{-3}$ | |
| 3.000μm | Base | $Al_{0.5}In_{0.5}P$ | $n=2e17\ cm^{-3}$ | |
| 0.500μm | BSF | $In_{0.5}(Al_{0.7}Ga_{0.3})_{0.5}P$ | $n=5e18\ cm^{-3}$ | |
| 0.200μm | Substrate | GaAs | $n=1e18\ cm^{-3}$ | GaAs Substrate |

Cathode Contact

**Fig. 2** Schematic of the proposed dual-junction cell

### 2.3. Simulation model

The performance of the proposed cell was simulated using Atlas the Silvaco Atlas within the standard of AM 1.5 (1 sun) spectrum and the results were compared with those from previous works. Figure 3 shows the meshing of the proposed cell. The areas were partitioned differently to accurately simulate the structure of the solar cell. In this model, QTX.MESH and QTY.MESH were used to calculate the quantum tunneling current. Figure 4 shows the energy band diagram of a dual junction cell with bias voltage of 0V.

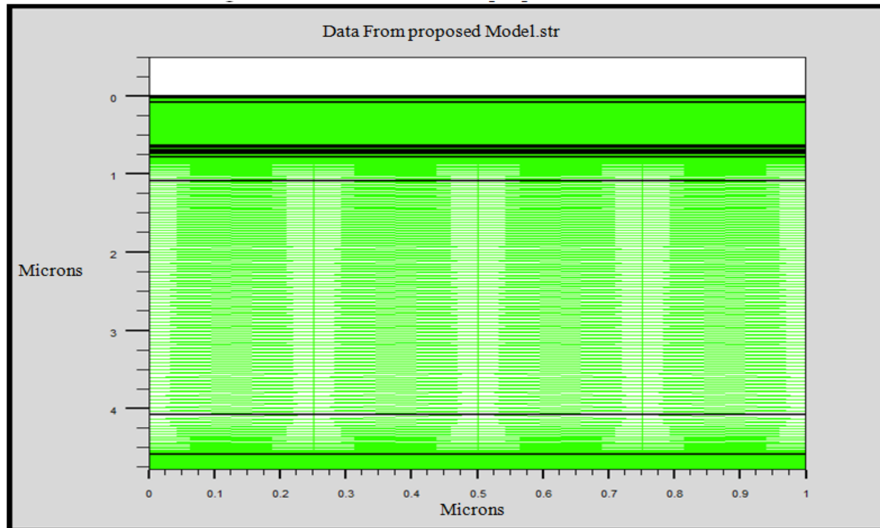


**Fig. 3** Generated mesh of the proposed dual-junction cell.

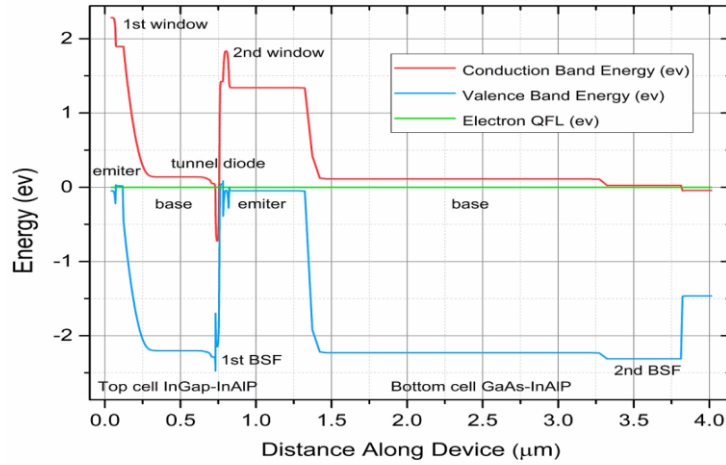


**Fig. 4.** Energy band diagram of the proposed model

## 3. Discussion and Results

### 3.1. Thickness and optimal impurity for upper and lower cells

P-n junction solar cell impurities in the emitter layer should be greater than in the base layer.The emitter layer is an absorbent layer in solar cells. To improve the performance of the solar cell, the thickness of this layer should be less than that of the base layer [15].

The thickness (emitter = 0.05, base = 0.55) (μm) and optimal impurity (emitter = $2\times10^{19}$, base = $7\times10^{16}$) ($1/cm^3$) are shown in Figures 5a and 5b for the InGaP/AlInPheterojunction. The thickness (emitter = 0.3, base = 3.0) (μm) and optimal impurity (emitter = $2\times10^{18}$, base = $2\times10^{17}$) ($1/cm^3$) are shown in Figures 6a and 6b for the GaAs/AlInPheterojunction.

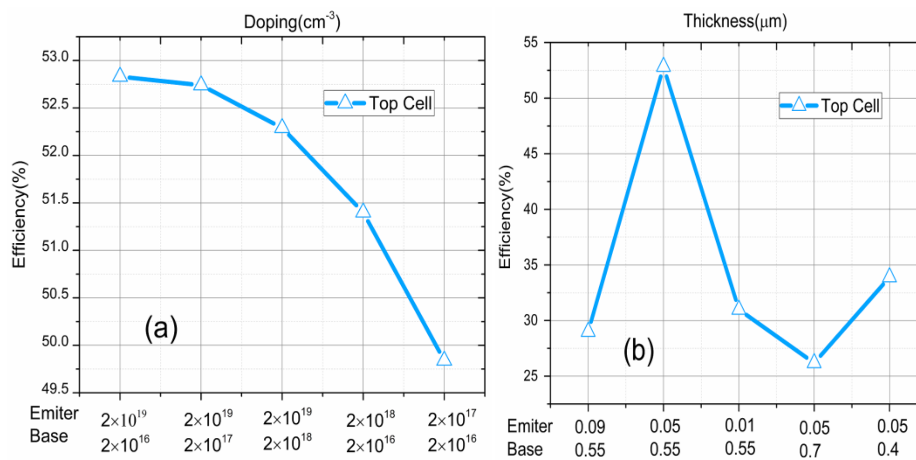


**Fig. 5** a) Different solar cell parameters with various doping of new top cell,
b) The different parameters obtained by varying the thickness of new top cell.

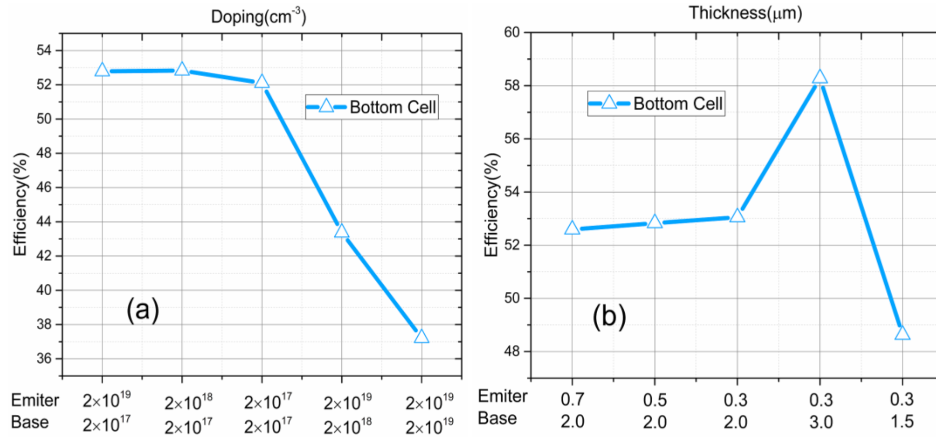


**Fig. 6** a) Different solar cell parameters with various doping of new bottom cell, b) The different parameters obtained by varying the thickness of new bottom cell.

### 3.2 Illumination with AM1.5G

Figures 7 and 8 show the optical intensity in the base cell [5] and proposed cell. Comparison of the optical intensity of the different layers indicates that the optical intensity of the proposed cell is less than that of the base cell due because of the increased absorption of photons in different layers. The value of the spectral response will determine solar cell gain and includes source photocurrent, available photocurrent and cathode current.

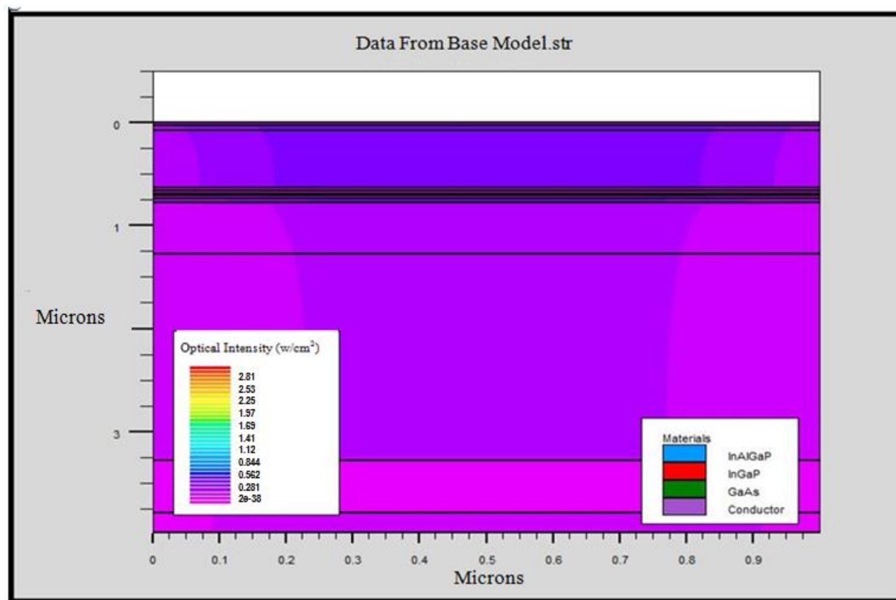


**Fig. 7** Optical intensity of different layers of the base model

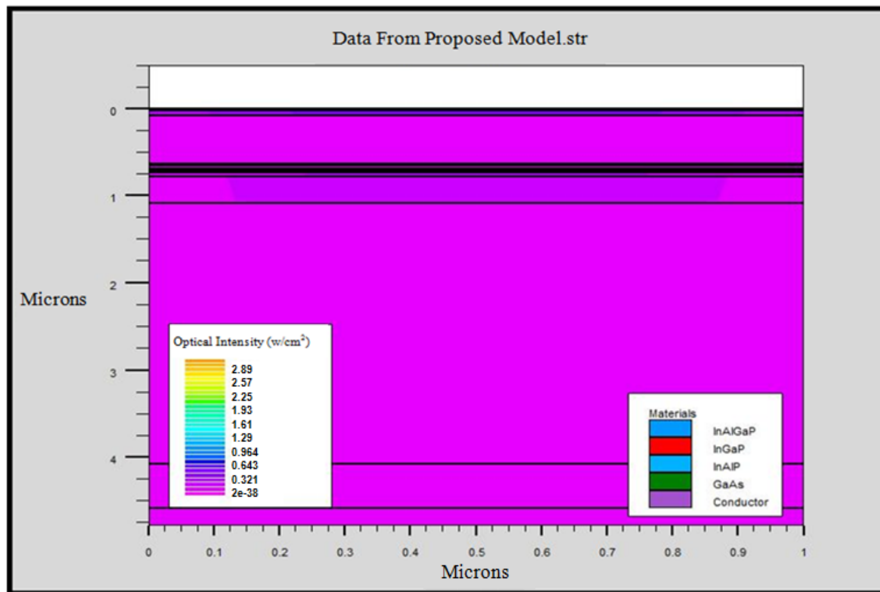


**Fig. 8** Optical intensity of different layers of the proposed model.

Source photocurrent is the amount of photons produced by the source photocurrent and available photocurrent. The cathode current measures photons absorbed in the solar cell and output current resulting from their absorption [15]. Figure 9 shows the absorbed photons and cathode current for InGaP and InGaP/AlInPcells and indicates that the amount of absorbed photons and cathode current in the InGaP/AlInP is greater. Figure 10 shows the absorbed photons and cathode current in the GaAs and GaAs/AlInP cells in which the amount of absorbed photons and cathode current in GaAs/AlInP is greater.

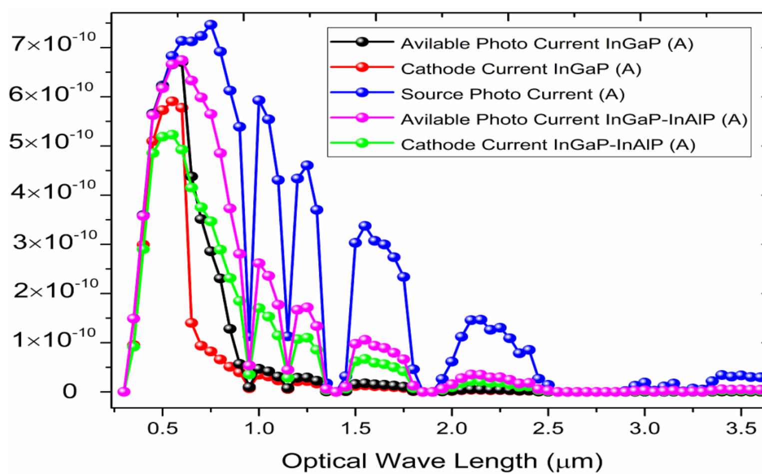


**Fig. 9** Generation of photocurrent by top cell of the base and proposed dual-junction cell

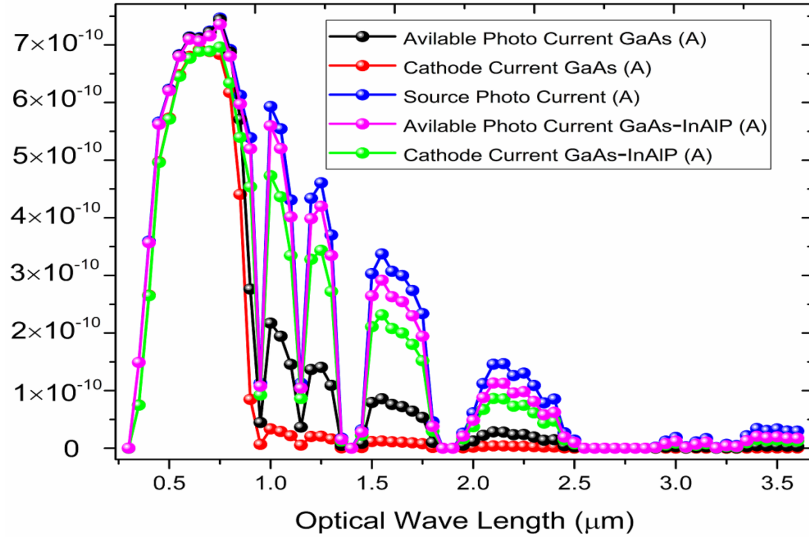


**Fig. 10** Generation of photocurrent by bottom cell of the base and proposed dual-junction cell

### 3.3. Photogeneration

Photogeneration shows amount of photons produced by sunlight in the different layers of a solar cell and is obtained as:

$$G = \eta 0 \frac{P\lambda}{hc} \alpha e^{-\alpha y} \tag{1}$$

where G is photo-generation rate, η0 is the internal quantum efficiency, P is the cumulative effect of reflections, transmissions and losses due, ⅄ is the wavelength, h is the Plank’s constant, c is the light speed, α is the absorption coefficient for each set of (n,k) and y is the relative distance[4].

Figures 11 and 12 show that photogeneration decreased from the top of the cell to the bottom due to the reduced absorption of photons in the lower layers. For example, in the base cell, photogeneration primarily occurring in the window layers at the top of the cell equaled $10^{22}$ electrons and holes per $cm^3$. This amount decreased to ~$10^{19}$ electrons and holes per $cm^3$ in the base layer at the bottom of the cell. Figure 13 shows photogeneration in the base and proposed cells. Comparison of the two cells indicates that photogeneration in the base layer at the tops and bottoms of the cells in the proposed model was caused by a reduction in the rate of recombination of electrons and holes produced and an increase in the absorption of photons after application of the InAlP semiconductor.

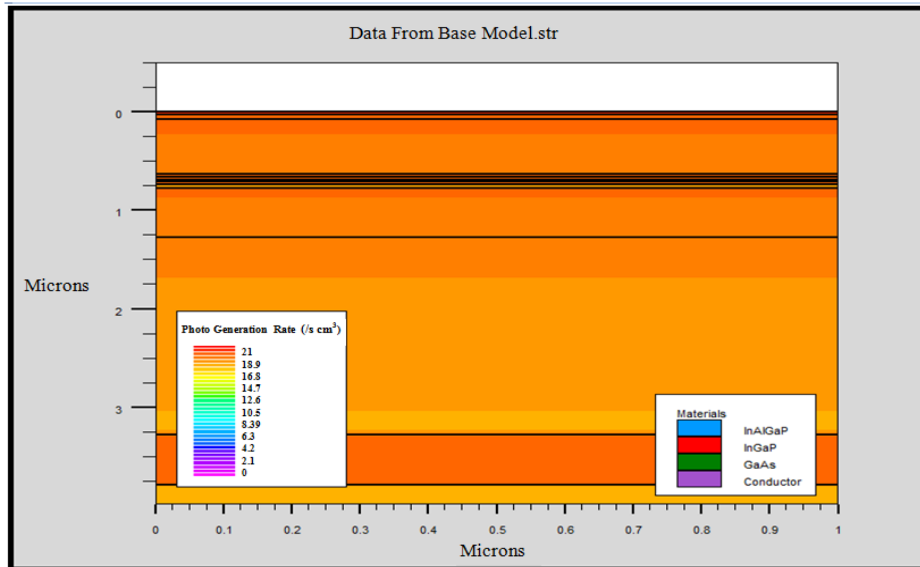


**Fig. 11** Photogeneration rate of the base model

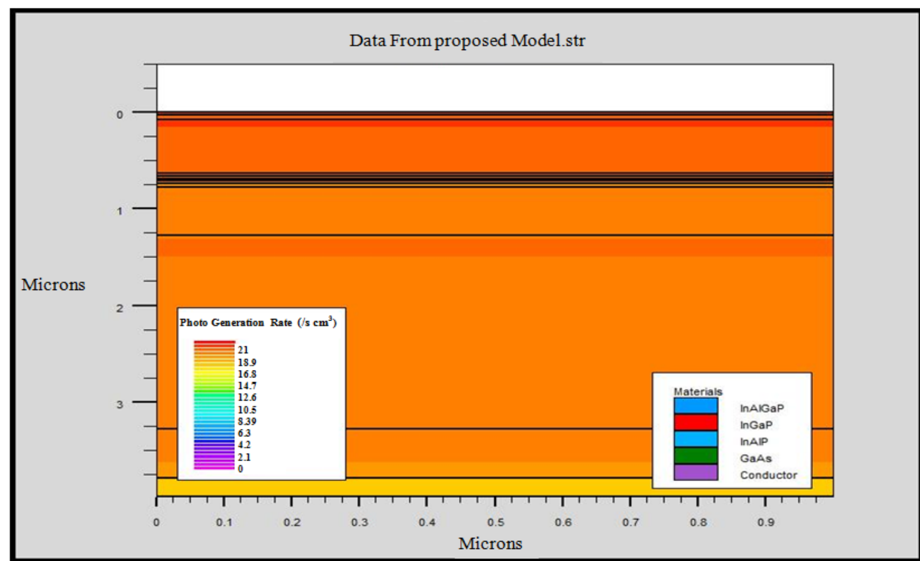


**Fig. 12** Photogeneration rate of the proposed model

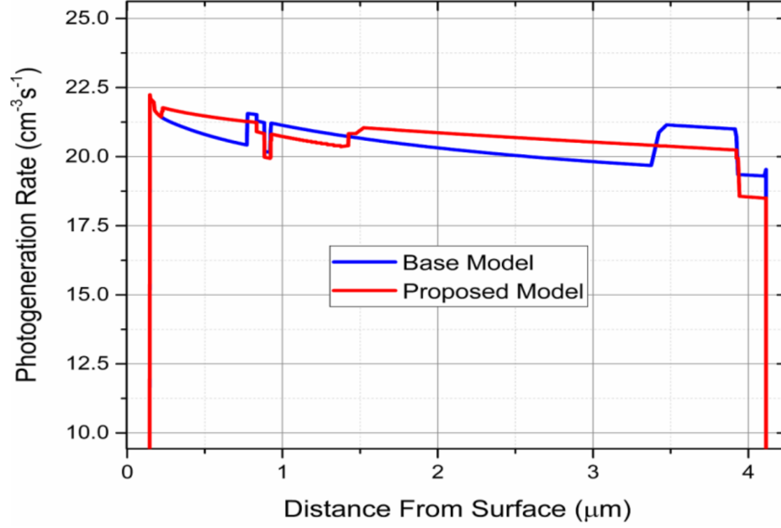


**Fig. 13** Cutline view of photogeneration rate of the base and proposed model

### 3.4. Important parameters in solar cells

*3.4.1. Short circuit current and open circuit voltage*

The total current in one solar cell is obtained as [4]:

$$I = I_0\left[\exp\left(\frac{qv}{nKT}\right) - 1\right] - I_L \tag{2}$$

where n is the diode in an ideal state, k is the Boltzmann constant, T is the temperature (K), q is the electrical charge, $I_L$ is the light generated current and $I_0$ is the current in a dark state. The open circuit voltage is obtained as [4]:

$$V_{oc} = \frac{nKT}{q}\mathrm{Ln}\left(\frac{I_l}{I_0} + 1\right) \tag{3}$$

*3.4.2. Fill factor*

The fill factor shows the maximum output power to ideal power in a solar cell and is obtained using the I-V curve. This factor is expressed in percent and is calculated as [16]:

$$FF = \frac{V_m \times I_m}{V_{OC} \times I_{sc}} \tag{4}$$

*3.4.3. Efficiency*

The performance of a solar cell is determined by the efficiency and is obtained as [16]:

$$\eta = \frac{P_{max}}{P_{in}} = \frac{V_m I_m}{P_{in}} \tag{5}$$

V-I curve for the proposed model is illustrated in figure 14.

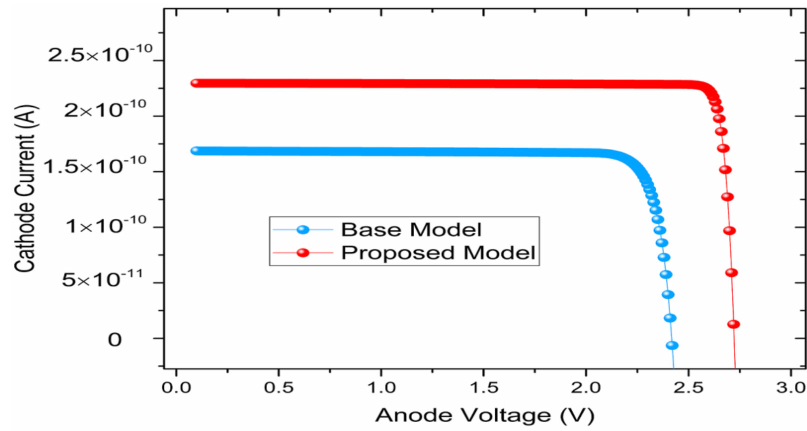


**Fig. 14** I-V curve of the base and proposed model

## 4. Comparison of Performance

The parameters of short circuit current, open circuit voltage fill factor and efficiency of the optimized model of the proposed cell were compared with results of other models in Table 2. In S. Abbasian et al [6], semiconductor $In_{0.5}(Al_{0.7}Ga_{0.3})_{0.5}P$ decreased in the cells, which increased the electrical field. This resulted in fewer recombinations; thus, the use of heterojunction GaAs/AlInPcells on the bottom reduced the recombination of cells and increased efficiency. As seen, the use of heterojunction InGaP/AlInP at the top and GaAs/AlInP at the bottom of a dual junction cell increased its efficiency.

**Table 2** Comparison of proposed model with the different optimized InGaP/GaAs DJ solar cell structures for spectrum AM 1.5G

| Solar cells | Spectrum | Sun | Voc(V) | Jsc (mA/cm$^2$) | FF (%) | η (%) |
|---|---|---|---|---|---|---|
| Lueck et al [2] | AM1.5G | 1.0 | 2.23 | 10.9 | 79.00 | 23.6 |
| Leem et al [3] | AM1.5G | 1.0 | 2.30 | 10.7 | 87.55 | 25.14 |
| Singh&sarkar [4] | AM1.5G | 1.0 | 2.39 | 16.1 | 87.52 | 32.196 |
| Nayak et al [5] | AM1.5G | 1000 | 2.66 | 17.3 | 88.67 | 39.15 |
| Dutta et al [17] | AM1.5G | 1000 | 2.668 | 18.2 | 88.29 | 40.879 |
| Sahoo et al [7] | AM1.5G | 1000 | 2.7043 | 18.9 | 88.88 | 43.603 |
| Abbasian et al [6] | AM1.5G | 1 | 3.347 | 17.5 | 90.90 | 53.51 |
| This model | AM1.5G | 1.0 | 2.72 | 22.9 | 93.26 | 58.28 |

## 5. CONCLUSION

In this design, short circuit current, open circuit voltage and fill factor increased due to changing the structure and replacing the InAlP semiconductor with band-gap of 2.4 ev in the base layer of the top and bottom cell of a GaInP/GaAsdual junction cell. The efficiency has been optimized by changing the thicknesses and the impurity density of the top and bottom layers. This optimized cell provides open circuit voltage (Voc) = 2.72 V, short circuit current (Jsc) = 22.96 mA/cm2, fill factor (FF) = 93.26% and efficiency (η) = 58.28% under radiation (1 sun).

## REFERENCES

[1] J.A. Hutchby, R J. Markunas, S.M. Bedair, "Material aspects of the fabrication of multi junction solar cells", In Proceedings of the 14th Critical Reviews of Technology Conference. Arlington, 1985, pp. 40-61.

[2] M.R. Lueck, C.L. Andre, A.J. Pitera, M.L. Lee, E.A. Fitzgerald, S.A. Ringel, "Dual junction GaInP/GaAs solar cells grown on metamorphic SiGe/Si substrates with high open circuit voltage", *IEEE Electron Device Lett.*, vol. 27, pp. 142-144, 2006.

[3] J.W. Leem, Y.T. Lee, J.S. Yu, "Optimum design of InGaP/GaAs dual-junction solar cells with different tunnel diodes", *Opt. Quantum Electron.*, vol. 41, pp. 605-612, 2009.

[4] K.J. Singh, S.K. Sarkar, "Highly efficient ARC less InGaP/GaAs DJ solar cell numerical modeling using optimized InAlGaP BSF layers", *Opt. Quantum Electron.*, vol. 43, pp.1-21, 2009.

[5] P.P. Nayak, J.P. Dutta, G.P. Mishra, "Efficient InGaP/GaAs DJ solar cell with double back surface field layer", *Eng. Sci. Technol. Int. J.*, vol.18, pp. 325-335, 2015.

[6] S. Abbasian, R. sabbaghi-Nadooshan, "Design and evaluation of ARC less InGaP/AlGaInP DJ solar cell", *Optik.*, vol. 136, pp. 487-496, 2017.

[7] G.S. Sahoo, P.P. Nayak, G.P. Mishra, "An ARC less InGaP/GaAs DJ solar cell with hetero tunnel junction", *Superlattices and Microstructures*, vol. 95, pp. 115-127, 2016.

[8] F.S.Gabibov, E.M. Zobov, "Effect of optical and thermal stimulation on GaAs photosensitivity", *Inorganic Materials,* vol. 49, no. 8, pp. 754–757, 2013.

[9] A.S. Gudovskikh, K.S. Zelentsov, N.A. Kalyuzhnyy, V.M. Lantratov, S.A. Mintairov, "Anisotype GaAs based heterojunctions for III-V multijunction solar cells", In Proceedings of the 25th European Photovoltaic Solar Energy Conference and Exhibition 2010.

[10] M.R. Islam, R.D. Dupuis, A.L. Holmes, A.P. Curtis, N.F. Gardner, G.E. Stillman, J.E. Baker, R. Hull, "Luminescence characteristics of InA1P-InGaP heterostructures having native-oxide windows", *Journal of Crystal Growth*, vol. 170, pp. 413-417, 1997.

[11] I. Vurgaftman, J.R. Meyer, L.R. Rammohan, "Band parameters for III-V compound semiconductors and their alloys". *J. Appl. Phys.*, vol. 89, pp. 5815, 2001.

[12] SILVACO Data Systems Inc, Silvaco ATLAS User's Manual, 2010.

[13] H.Y. Lee, C.T. Lee, "The investigation for various treatments of InAlGaP Schottky diodes",In Proceedings of the 8th International Conference on Electronic Materials, IUMRS-ICEM 23, 2002, pp. 99-102.

[14] P. Michalopoulos, "A novel approach for the development and optimization of state-of-the-art photovoltaic devices using silvaco", Naval Postgraduate School Monterey, California, 2002.

[15] A. Luque, S. Hegedus, Handbook of Photovoltaic Science and Engineering, England, John Wiley & Sons Ltd., 2003 , pp. 83-87.

[16] S. M. Sze, M. K. Lee, .Semiconductor Devices Physics and Technology, Wiley 2010

[17] J.P. Dutta, P.P. Nayak, G.P. Mishra, "Design and evaluation of ARC less InGaP/GaAs DJ solar cell with InGaP tunnel junction and optimized double top BSF layer", *Optik.*, vol. 127, pp. 4156-4161, 2007.